International Journal of Minerals, Metallurgy and Materials
Volume 23, Number 7, July 2016, Page 751
DOI: 10.1007/s12613-016-1289-x

Phosphorus partitioning and recovery of low-phosphorus iron-rich compounds through physical separation of Linz-Donawitz slag

Dilip Makhija[1)], *Rajendra Kumar Rath*[2)], *Kaushik Chakravarty*[1)], *Abhay Shankar Patra*[1)], *Asim Kumar Mukherjee*[1)], *and Akhilesh Kumar Dubey*[3)]

1) Research and Development Division, Tata Steel Ltd., Jamshedpur, 831001, India
2) Mineral Processing Division, CSIR-National Metallurgical Laboratory, Jamshedpur, 831007, India
3) Raw Material Blending and Bedding Section, Tata Steel Ltd., Jamshedpur, 831001, India
(Received: 29 October 2015; revised: 27 January 2016; accepted: 22 February 2016)

Abstract: The Linz-Donawitz (LD) steelmaking process produces LD slag at a rate of about 125 kg/t. After metallic scrap recovery, the non-metallic LD slag is rejected because its physical/chemical properties are unsuitable for recycling. X-ray diffraction (XRD) studies have indicated that non-metallic LD slag contains a substantial quantity of mineral phases such as di- and tricalcium silicates. The availability of these mineral phases indicates that LD slag can be recycled by iron (Fe)-ore sintering. However, the presence of 1.2wt% phosphorus (P) in the slag renders the material unsuitable for sintering operations. Electron probe microscopic analysis (EPMA) studies indicated concentration of phosphorus in dicalcium silicate phase as calcium phosphate. The Fe-bearing phases (i.e., wustite and dicalcium ferrite) showed comparatively lower concentrations of P compared with other phases in the slag. Attempts were made to lower the P content of LD slag by adopting various beneficiation techniques. Dry high-intensity magnetic separation and jigging were performed on as-received samples with particle sizes of 6 and 3 mm. Spiral separation was conducted using samples ground to sizes of less than 1 and 0.5 mm. Among these studies, grinding to 0.5 mm followed by spiral concentration demonstrated the best results, yielding a concentrate with about 0.75wt% P and 45wt% Fe.

Keywords: steelmaking slag; dephosphorization; recycling

1. Introduction

A large quantity of solid waste is generated during iron (Fe)- and steelmaking, of which basic oxygen furnace (BOF) slag or Linz-Donawitz (LD) slag accounts for a fairly significant fraction [1–2]. LD slag, a by-product of the steel industry, comes from pig Fe refinement using an LD converter [3]. The production of 1 t of steel during pig Fe conversion generates roughly 100 kg of slag depending on the pig Fe composition, required quality of steel, and conversion process applied [4].

The LD slag is highly basic and may contain up to 25wt% metallic Fe. Other mineral phases in this slag include free lime, dicalcium aluminoferrite, wustite, and dicalcium silicate [4]. The presence of minerals such as periclase, manganosite, Fe and Mn monticellite, Mn cordierite, and glass has also been reported [5]. At Tata Steel Ltd., India, the metallic components of LD slag are recovered through a series of crushing and magnetic separation procedures. Magnetic separation recovers about 25% of the total mass of LD slag as a magnetic product.

The non-magnetic fraction of the crushed slag, which is usually 6 mm in size, is either stored or utilized as an aggregate for road making. Although this non-magnetic fraction does not contain a large amount of metallic Fe, it contains a substantial quantity of calcium-bearing mineral phases such as di- and tricalcium silicates. The rejects also contain useful components such as CaO and MgO, which present high basicities of above 3. It is not stable volumetri-

Corresponding author: Dilip Makhija E-mail: d.makhija@tatasteel.com; maki14@rediffmail.com

cally because of hydration tendency of CaO and MgO, which ultimately results in expansion and cracking [6–7].

LD slag features a high fluxing capacity due to the presence of dicalcium and tricalcium silicate and is charged in blast furnaces because of its easy melt ability and potential utilization of calcium [3]. In addition to calcium phases, Fe in LD slag is present as Fe (metallic), calcium ferrites, and wustite containing MgO and MnO; thus, the slag can be used in Fe ore sintering [8]. However, the presence of high phosphorus (P) content in the LD slag renders it unsuitable for industrial applications [9].

Extensive research work has been carried out over the last 40 years to explore techniques that will allow utilization of bulk LD slag. When properly treated, LD slag may be used as aggregates for road construction and hydraulic engineering, fertilizers [3,10], and feeds for Fe ore sintering and BOF to utilize its useful elements, which include Fe, Mn, CaO, and MgO [5,11–12]. However, utilization of the slag in civil engineering applications is difficult because of its poor volume stability attributed to the presence of free lime [13].

The stringent quality control of finished steel has restricted the quantity of LD slag that can be utilized in recycling applications. The most harmful components of LD slag are P and sulfur (S), which must be removed from the material before its use either in sintering plants or blast furnaces. The use of LD slag in Bhilai Steel Plant, India, was discontinued because of the high P and S contents of the material [14]. The prevailing level of 3wt%–4wt% P_2O_5 in LD slag is too high for recycling in sintering and blast furnace processes. To address this problem, several extensive studies have been carried out. Two reported methods for P reduction include evaporation [15–17] and floating [18]. The use of a strong magnetic field to recover crystalline phases containing P element has also been reported [19]. Reports reveal that 50wt% P in the initial slag could be recovered by a magnetic field gradient of around 2 T. Recent studies conducted on LD slag containing 18.1wt% Fe, 45.9wt% CaO, 20.3wt% SiO_2, 6.6wt% P_2O_5, 2.5wt% MnO, and 5.5wt% MgO with a superconducting magnet of 0.5–2.5 T show that the recovery of P phases decreases with increasing particle size of the ground slag [20].

Research works on P reduction through bioleaching or chemical leaching have also been conducted, but these processes are either very slow (bioleaching) or very costly (chemical leaching). Alternative approaches to LD slag utilization, such as CO_2 sequestration, have been attempted, and results indicate that 6vol%–11vol% of the CO_2 generated from the LD vessel can be sequestered [21]. Physical separation of P has been also attempted by adopting a flotation technique, but this process is unable to lower the P in steel slag significantly.

In this study, an attempt was made to explore a cost-effective technique to achieve a P content of less than 1wt% in LD slag. Physical separation techniques with and without grinding of the LD slag were explored to render it suitable for recycling via Fe ore sintering as a flux substitute.

2. Experimental

2.1. Material and characterization

LD slag samples with sizes below 6 mm were collected from the waste recycling plant stockpile. This fraction was generated during metal recovery from LD slag. The cooling and metallic recovery process consisted of pouring the molten LD slag into a pit followed by sprinkling of water over the top of the slag. The water-quenched LD slag was then allowed to slowly cool for a period of 24–30 h after which it was crushed using steel balls. Crushing is done to reduce the slag sample to particles with sizes of less than 300 mm. After crushing to 300 mm, magnetic separation of the coarse metallic particles was performed. A second cycle of crushing of the non-metallic component of the 300 mm slag to less than 80 mm in size, followed by magnetic separation, was then performed. Finally, a third cycle of crushing of the 80 mm non-metallic particles to less than 6 mm, followed by magnetic separation, was performed. The non-magnetic fraction of particles with sizes of less than 6 mm, which was made up about 75wt% of the total steel slag, was taken for P removal studies. A total of three samples were collected to represent the entire slag stockpile.

The average chemical composition of the head sample revealed contents of 18.3wt% Fe, 43.8wt% CaO, 14.9wt% SiO_2, 2.9wt% Al_2O_3, and 1.2wt% P. The chemical analysis results of the head sample are shown in Table 1.

Table 1. Chemical composition of LD slag head sample

wt%

Fe(T)	FeO	CaO	SiO_2	Al_2O_3	MgO	P
18.3	13.3	43.8	14.9	2.9	4.7	1.2

The main constituents of LD slag are Fe, CaO, SiO_2, Al_2O_3, and MgO. The presence of high CaO contents can be attributed to lime that was used to slag out SiO_2 and other impurities during steelmaking. CaO was mostly present in the form of dicalcium silicate and calcium aluminoferrite. The oxidizing atmosphere used during steelmaking oxidizes

the metallic Fe, which subsequently reacts with the lime and aluminates to form calcium aluminoferrite. The LD slag also contained about 1.2wt% P, which was present in the form of phosphate. The calcium phosphate observed was mostly associated with dicalcium silicate.

The chemical analysis results of the LD slag sample separated according to size presented in Table 2 indicate that coarser fractions contain more Fe-bearing minerals than finer ones. Fractions with particle sizes below 0.075 mm contained 11.94wt% Fe in comparison with the average sample Fe content of 18.3wt%. The distribution of P is higher in coarse fractions than in fine ones. Finer fractions, e.g., samples sized 0.1 mm and below, revealed less than 1wt% P. The size-wise analysis suggests that size classification of the sample at about 0.1 mm to separate +0.1 mm from –0.1 mm can lower the P content in –0.1 mm fraction to less than 1wt%. However, the concentrate yield in this case would only be about 11wt%.

Table 2. Size wise chemical analysis of LD slag

Size / mm	Weight / %	Chemical composition						
		Fe(T)	FeO	SiO_2	CaO	Al_2O_3	MgO	P
+6	13.8	17.88	18.06	13.96	44.45	2.04	3.74	1.18
+3	18.6	20.92	20.64	14.03	44.57	3.38	4.54	1.22
+1	22.2	21.01	20.64	15.30	43.62	2.79	4.06	1.17
+0.5	4.9	20.53	26.49	15.95	40.84	2.73	5.12	1.02
+0.25	25.1	16.67	12.77	15.40	43.00	2.48	5.55	1.02
+0.15	4.1	14.52	12.90	15.04	41.75	2.11	6.39	1.12
+0.10	3.3	15.43	11.87	14.15	44.15	2.28	5.22	0.866
+0.075	3.3	15.44	10.32	12.67	41.40	2.66	5.20	0.718
–0.075	4.7	11.94	7.22	12.95	42.79	3.38	6.01	0.482
Total	100							

2.2. Mineralogical properties of steel slag

X-ray diffraction (XRD) studies of LD slag were carried out to understand the types of mineral phases present in the slag. These studies revealed that the major phases present in the LD slag included dicalcium silicate ($2CaO{\cdot}SiO_2$), wustite (FeO), tricalcium silicate ($3CaO{\cdot}SiO_2$), calcium aluminoferrite ($Al_{0.6}Ca_2Fe_{1.4}O_5$), magnesioferrite ($Fe_{0.6}Mg_{0.24}O$), and free lime (CaO). An XRD pattern of the slag is shown in Fig. 1.

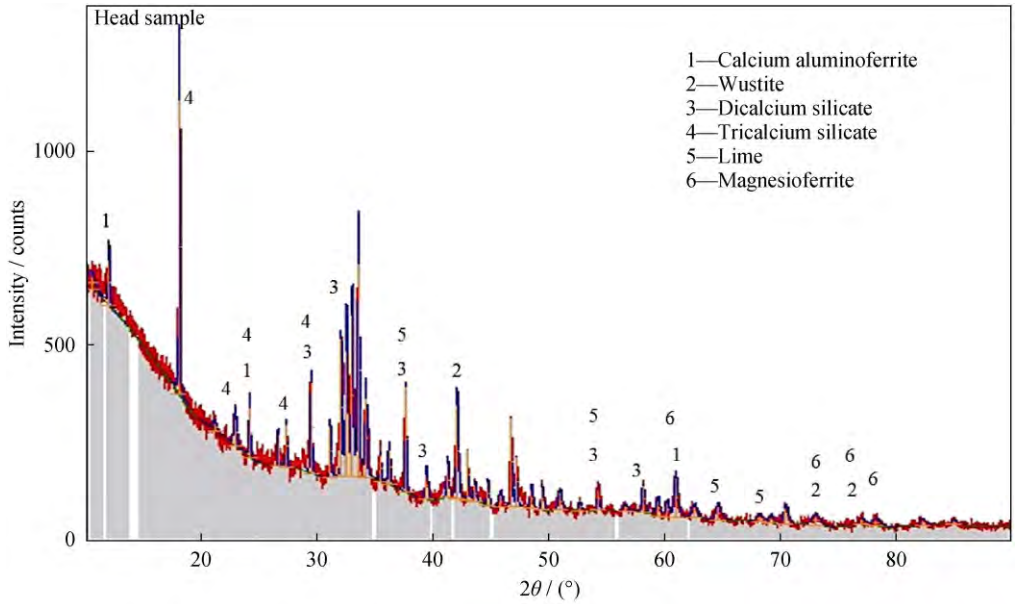

Fig. 1. XRD pattern of LD slag.

An electron probe microscopic analysis (EPMA) study was carried out to understand the elemental distribution in various phases of the slag as well as the associations of P. Preliminary identification of the phases present in the slag was carried out by EPMA at three different areas in two samples. Figs. 2 and 3 show the focal points of analysis in the samples, and Tables 3 and 4 show the compositions of these points. Here, calcium ferrite was categorized into three varieties: (a) CaO and FeO contents of nearly equal proportion (47wt% and 45wt%) with a large amount of alumina (~7wt%), (b) high FeO (68wt%) and comparatively low CaO (22wt%) contents with magnesia (~9wt%) and MnO (~1wt%), and (c) high CaO (~48wt%) and low FeO (~35.5wt%) contents with TiO_2 (~7wt%), alumina (~6wt%), and silica (~2wt%). Other major phases present in the given slag included dicalcium silicate. The phosphate concentration is notably higher in dicalcium silicate phase (ranging from 2wt% to 8wt%) than in other phases. Steel slag seldom forms a glassy phase even at very high cooling rates. Crystal formation is a function of both cooling rate and the chemical composition of steel slag. The slowly cooled slag in our study presented a crystal size between 50–150 μm. Reddy *et al*. [22] also identified a highly crystalline structure in quenched BOF slag by using XRD analysis. These studies indicate that, even when rapidly cooled, in general, steel slag tends to crystallize because of its chemical composition. The phosphate in slowly cooled slag tends to accumulate in the larger crystals of dicalcium silicate (5wt%–7wt%), while Fe-rich phases show comparatively lower concentrations of phosphate (less than 1wt%). The presence of metallic Fe may also be observed in Fig. 3 as point 1, the elemental analysis result of which is shown in Table 4.

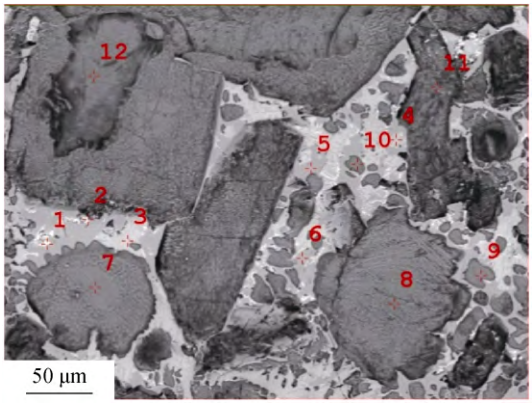

Fig. 2. EPMA image of LD slag.

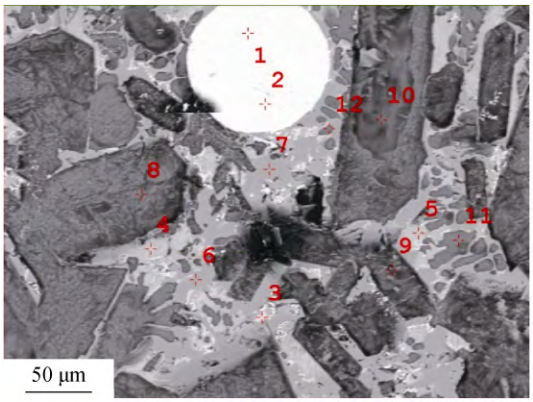

Fig. 3. EPMA image of LD slag.

Table 3. Elemental analysis of different phases corresponding to Fig. 2 wt%

Point	SiO_2	Al_2O_3	MgO	CaO	FeO	MnO	P_2O_5	Phase
2	16.20	0.76	0.49	57.23	22.10	0	2.55	Ca–Fe silicate
3	0	0.09	8.57	22.40	67.58	1.23	0.12	Ca–Mg–Fe
4	0.01	0	16.60	1.90	79.12	2.18	0.08	Mg–Fe oxide
9	27.75	0.55	0	63.92	1.64	0	5.41	Ca–Si
10	25.84	0.65	0	64.94	1.94	0.02	5.87	Ca–Si
11	24.85	0.63	1.25	65.62	5.18	0.09	2.00	Ca–Si

2.3. Methods

2.3.1. Dry high-intensity magnetic separation

Separation of metallic Fe and minerals from LD slag using magnetic techniques has been widely reported in the literature. A cross-belt magnetic separator, drum magnetic separator, and magnetic pulley separator are usually used for separation work. The results reported by Wu *et al*. [23] show that P in steel slag occurs predominantly in dicalcium silicate and, to a lesser extent, in dicalcium ferrite in solid solutions. Dry high-intensity magnetic separation (DHIMS) was used to separate the P-bearing dicalcium silicate from the Fe-bearing minerals. It was reported that cooling rate is an important parameter to consider in slag treatment [24]. According to these authors, higher yields of the Fe-bearing concentrate are obtained when the slag is slowly cooled. This finding can be explained by increases in the amount and size of the crystalline phases and decreases in the glass matrix during the slow cooling of the liquid slag. In our research work, DHIMS was performed on samples crushed to

3 and 6 mm to separate the Fe-rich compounds from the calcium-rich dicalcium silicate compounds. The tests were conducted in a rare earth roll magnetic separator with a magnetic intensity of about 15000 Gs at the roll surface. The feed rate and roll speed were varied to achieve yield–grade plots from different parameters.

Table 4. Elemental analysis of different phases corresponding to Fig. 3 wt%

Point	SiO_2	Al_2O_3	MgO	CaO	Fe	FeO	MnO	P_2O_5	Phase
1	0.03	0	0.01	0	99.89		0.02	0.01	Fe
2	0.06	0.03	0	0	99.88		0	0	Fe
4	0	0	14.32	7.85		75.99	1.80	0	Mg–Fe oxide
5	0	0.02	8.88	21.46		68.24	1.26	0.04	Calcium ferrite 2
6	1.77	5.50	0.48	48.49		33.57	0.08	0.65	Calcium ferrite 3
8	25.01	0.70	1.64	62.51		7.08	0.26	2.32	Ca–Si
11	24.18	0.49	0.09	65.96		1.78	0.01	6.68	Ca–Si
12	21.36	1.06	0.15	64.38		3.07	0.03	7.92	Ca–Si

2.3.2. Jigging (mineral density separation)

Jigging tests were conducted in a mineral density separator (MDS). The MDS is capable of stratifying an ore sample according to differences in particle density. MDS tests were conducted with as-received 6 mm samples as well as with samples crushed to 3 mm. The test products were collected as two different-density fractions, i.e., a lighter fraction and a heavier fraction. The two layers were separately collected, dried, weighed, and analyzed for Fe and P, and a grade–yield plot was drawn.

2.3.3. Spiral separation

The 6 mm LD slag sample was divided into two representative samples through coning and quartering. Each of the 6 mm samples was then individually stage-crushed to 100% passing 1 and 0.5 mm. Stage-crushed samples of 1 and 0.5 mm were then individually subjected to spiral separation. The spiral tests were conducted by varying the splitter position to obtain a yield–grade plot of the concentrate. The solids in feed were maintained at 15wt% throughout all of the tests. The feed rate of dry solids was maintained at 100 kg/h for all tests. The spiral products, i.e., the concentrate, middling, and tailing, were separately collected, dried, weighed, and analyzed for Fe and P to understand the effect of concentrate yield on the quality of the final concentrate.

3. Results and discussion

3.1. Dry high-intensity magnetic separation

DHIMS of the 6 mm as-received sample was conducted at different roll speeds, resulting in a magnetic concentrate yield varying from 43.8% to 81.4% and slightly richer Fe values in the concentrate. The Fe content varied linearly and inversely with the yield of the concentrate, and a maximum value of 21.9wt% Fe was achieved with a yield of about 43.8%. At a higher yield of 81.4%, the Fe content dropped to 19.5wt%. The results of DHIMS are shown in Fig. 4.

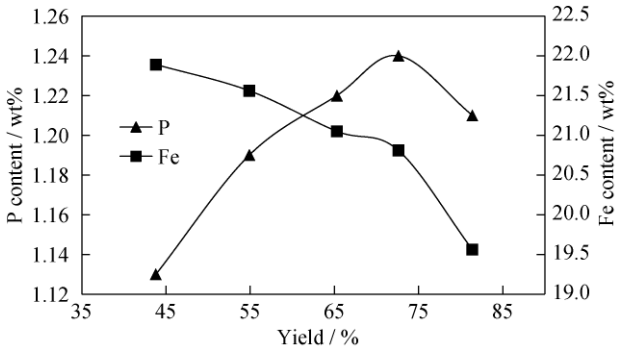

Fig. 4. Yield–grade plot of DHIMS of as-received LD slag crushed to 6 mm.

The P content of the magnetic concentrate of particles of 6 mm varied over a narrow range of 1.13wt%–1.24wt%. The P split in the concentrate and tailing was nearly equal at higher concentrate yields but slightly improved (i.e., lower P in the concentrate) at lower yields.

The yield–grade plot (Fig. 5) of 3 mm particles subjected to magnetic separation showed a maximum achievable Fe content of about 24wt%. The gradient of the yield–grade plot of 3 mm particles subjected to DHIMS is steeper compared with that of the 6 mm as-received sample. A steeper curve indicates a lower decrease in yield for every incremental increase in Fe in the concentrate. The Fe content in the concentrate of 3 mm particles was slightly higher than that obtained from the concentrate of 6 mm particles. Such a result can be attributed to the improved liberation of heavy Fe-rich minerals from lighter calcium-rich minerals in the 3 mm sample.

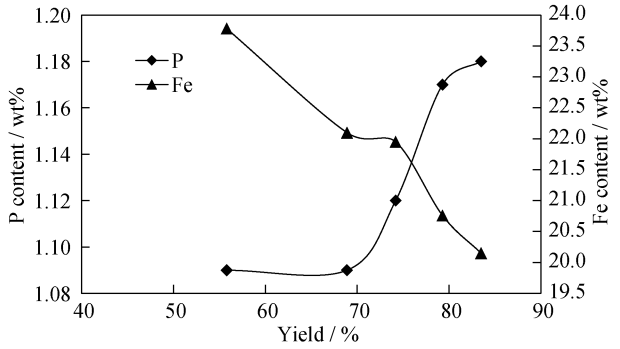

Fig. 5. Yield–grade plot of DHIMS of as-received LD slag crushed to 3 mm.

Particles of 3 mm revealed P contents in the range of 1.09wt%–1.18wt%. The effect of feed size was evident from the DHIMS results of the 3 mm sample, which showed lower P values compared with samples of other sizes. These results imply that reduction of the particle size of the DHIMS feed produces a marginal increase in the liberation of Fe- and P-rich compounds. However, the presence of more than 1wt% P in the magnetic concentrate renders the concentrate unsuitable for recycling applications. With only a marginal increase in the liberation of Fe-rich compounds at 3 mm, a particle size of less than 3 mm is required to achieve a P level of less than 1wt%.

The non-magnetic fraction of 6 mm particles subjected to DHIMS revealed about 17wt% Fe. The non-magnetic fraction, as seen in Fig. 6, contained a substantial quantity of Fe-bearing minerals, likely because of the poor liberation of Fe. Even at a particle size of 3 mm, DHIMS was unable to substantially lower the Fe content in the non-magnetic tailing.

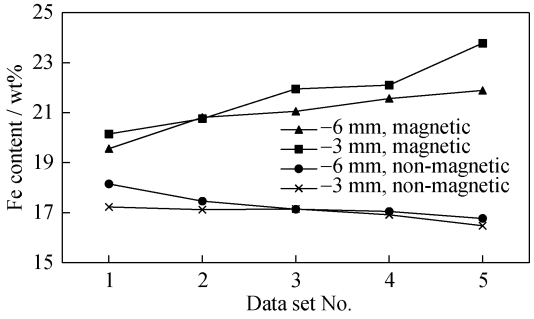

Fig. 6. Fe content of DHIMS of 6 and 3 mm particles.

The results of DHIMS indicate that separation of phosphate-rich phases (i.e., di- and tricalcium silicate) from phosphate-deficient phases is not possible under coarser particle sizes. However, a marginal reduction in P may be observed from the magnetic fraction at a particle size of 3 mm when compared with the results of the 6 mm sample. EPMA indicated a crystal size of 50–150 μm; thus, to achieve perfect separation of the dicalcium silicate phase from Fe-rich phases, the sample must be ground to these sizes. Research work conducted by Yokoyama *et al*. [19] indicated the preferential recovery of P-containing phases in the non-magnetic fraction; here, the size of the sample used was in the range of 70 μm and below. While the cooling pattern of the slag was not mentioned in this study, industrial practices reveal that slag is cooled over a period of 18–24 h, similar to the methodology in our case. The composition of the slag was also fairly constant. Therefore, the results of the cited research work can be generalized and extended to similar types of slag (e.g., steel slag). The role of particle size is of utmost importance in recovering P from non-magnetic fractions. A particle size of 50–150 μm, which is the crystal size range in the present study, is likely to result in substantial rejection of P in the non-magnetic fraction.

3.2. Jigging (mineral density separation)

Jigging tests were conducted in a mineral density separator. Jigging of the 6 mm as-received sample resulted in a concentrate yield of 28.9%–51.2%. The related results are shown in Fig. 7. The jigging concentrate, i.e., the heavier fraction, was enriched in Fe, the contents of which varied linearly and inversely with the concentrate yield. A maximum value of 24.5wt% Fe was achieved at a yield of about 28.9%. At higher heavy concentrate yields, Fe contents decreased linearly and inversely relative to the yield. The jigging concentrate did not show significant reductions in P. A minimum value of 1.18wt% P was obtained at a corresponding yield of 28.9%.

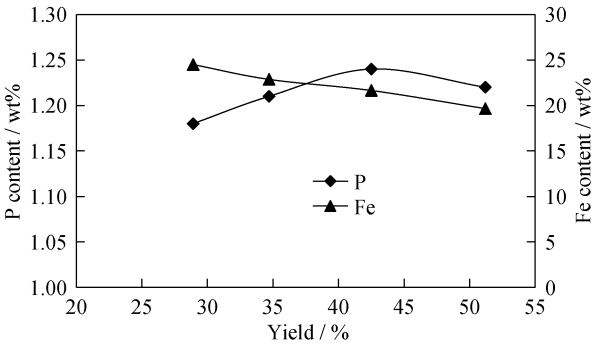

Fig. 7. Yield–grade plot of jigging of 6 mm particles.

The yield–grade plot of 3 mm samples subjected to jigging is shown in Fig. 8. The figure shows that the maximum achievable Fe content is about 28.5wt% at a yield of about 22%. The P of the jigging concentrate varied over a narrow range from 1.06wt% to 1.16wt% in the case of 3 mm particles. The P split in the concentrate and tailing was nearly

equal at higher concentrate yields but slightly improved (i.e., lower P in the concentrate) at lower yields. The effect of feed size was evident from the jigging results of the 3 mm sample, which showed slightly better separation of P compared with the other sample sizes.

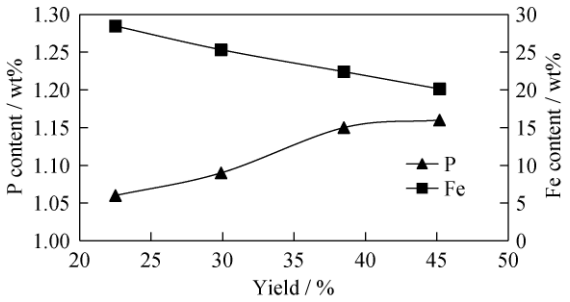

Fig. 8. Yield–grade plot of jigging of 3 mm particles.

The tailings of 6 and 3 mm particles subjected to jigging showed 15wt%–17wt% Fe. The tailing fraction contained a substantial quantity of Fe-bearing minerals, as evidenced by the high assay values obtained. The presence of Fe in the jigging tailings is attributed to the poor liberation of dicalcium aluminoferrite and wustite phases from the dicalcium silicate phase.

Compared with the results of DHIMS, jigging showed slight improvements in Fe level upgrade and P rejection from the concentrate. The upgrade observed, however, is inadequate to render the concentrate suitable for Fe ore sintering, which requires less than 1% P.

3.3. Spiral separation

Spiral separation studies were conducted with samples crushed to 1 and 0.5 mm. The concentrate yield was varied by changing the splitter position. Samples were drawn from the concentrate and analyzed for Fe and P, and the concentrate yield was plotted against the Fe content and P content obtained. The related plots are shown in shown in Figs. 9 and 10.

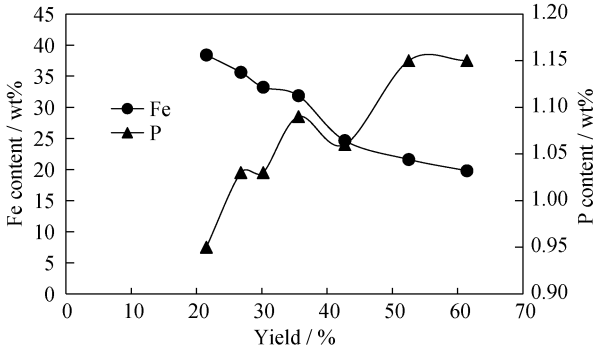

Fig. 9. Yield–grade plot of spiral separation of 1 mm particles.

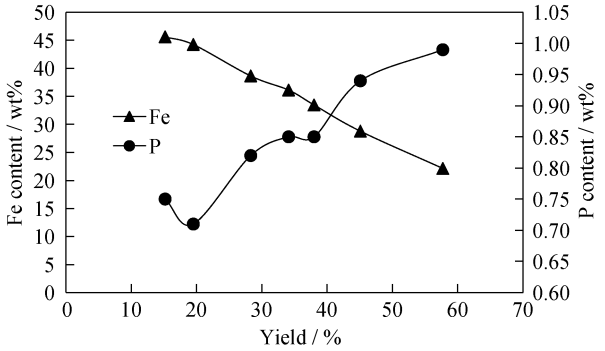

Fig. 10. Yield–grade plot of spiral separation of 0.5 mm particles.

Spiral separation of the 1 mm sample resulted in a concentrate yield ranging from 20% to 60% (Fig. 9). The spiral concentrate, which is a heavy fraction, was enriched in Fe. A maximum value of about 38wt% Fe was achieved at a yield of about 21%. Higher concentrate yields resulted in a linear reduction in Fe.

The yield–grade plot for spiral separation of the sample crushed to 0.5 mm is shown in Fig. 10. In the figure, the maximum achievable Fe content is about 45wt% at a yield of about 15%. The plot of the yield of 0.5 mm particles shows better separation compared with that of the 1 mm sample. At a similar Fe content of about 38wt%, the yield obtained from the 0.5 mm sample is about 28% whereas that obtained from the 1 mm sample is 21%.

The P content in the spiral concentrate varied between 0.95wt% and 1.15wt% in the case of the 1 mm sample. P recovery in the 1 mm tailings indicates that that the element is recovered more extensively in the tailing fraction of samples subjected to spiral separation than in those obtained through DHIMS and jigging. The results also suggest that liberation of phosphate in the dicalcium silicate phase is more extensive in particles of 1 mm than in particles of 6 or 3 mm.

Particles with a size of 0.5 mm revealed P contents in the range of 0.75wt%–1wt%. The effect of feed size was evident in the spiral test results of the 0.5 mm sample, which showed further reductions in P in the concentrate. The spiral concentrate obtained from 0.5 mm particles showed a better trade-off between yield and P content.

A high concentration of Fe-rich phase and a comparatively lower silica concentration in the spiral concentrate is an indicator that crystalline phases, such as wustite and dicalcium aluminoferrite, were preferentially separated in the concentrate. The presence of a large amount of silica and calcium in the spiral separation tailing product indicates that the large-sized crystals were mostly dicalcium silicates. Microscopic analysis revealed that wustite and calcium ferrite crystals are comparatively smaller than dicalcium silicate

crystals. Therefore, spiral separation results in segregation of these smaller crystals in the heavier fraction, while the glassy phase and larger crystals of dicalcium silicate are segregated in the tailing. However, since the liberation size of metallic Fe, wustite, and dicalcium aluminoferrite is very low (about 50–150 μm), it requires very fine grinding of the slag to efficiently separate iron bearing phases from the phosphate rich calcium bearing phases. Therefore, the separation efficiency (SE) of these phases is not very high. Thus, the separation of crystalline phase from the glassy phase is not perfect and both these phases report to concentrate as well tailing of spiral separation. However, a preferential separation of P rich phases is seen in spiral tailing which is evidenced from the presence of comparatively higher P in spiral tailing.

3.4. Separation efficiency of DHIMS, jigging, and spiral separation

The SE values of DHIMS, jigging, and spiral separation are compared. The SE may be calculated according to the following formula:

$SE = R_m - R_g$,

where R_g is the recovery of P in the concentrate, and R_m is the recovery of Fe in the concentrate.

$$R_m = \frac{\text{Concentrate yield} \times \text{Fe content in the concentrate}}{\text{Fe content in feed}} \times 100\%,$$

$$R_g = \frac{\text{Concentrate yield} \times \text{P content in the concentrate}}{\text{P content in feed}} \times 100\%.$$

A box plot of the SE values obtained from the different techniques is shown in Fig. 11.

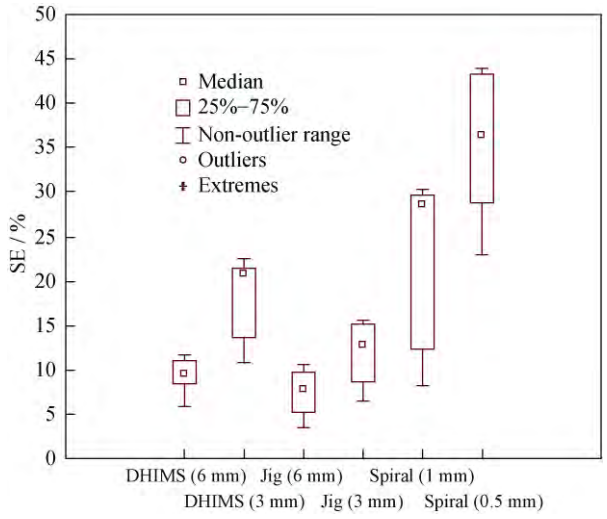

Fig. 11. Box plot of the separation efficiencies obtained from different techniques.

The SE of DHIMS using 6 mm particles varied from 6% to 12%. While the recovery of Fe was high in this procedure, the corresponding SE was low, probably because of the simultaneous recovery of gangue minerals (P) in the concentrate. DHIMS using 3 mm particles resulted in comparatively better SE values ranging from 11% to 23%.

The SE values of jigging using 6 mm particles varied from 4% to 11%, even lower than those obtained for DHIMS. The concentrate yield of DHIMS was clearly much higher than that of jigging, likely because of the presence of unliberated Fe oxide (wustite) along with other phases in the sample. Magnetic seeds of wustite in unliberated slag particles act as a center of attraction for the complete particle. Thus, even though the particles were smaller, the exposed wustite phase was attracted to the magnet, thereby increasing the yield and recovery of Fe. The SE values of jigging improved slightly (varying from 7% to 15%) when the sample was crushed to 3 mm. This result suggests that Fe in the slag is more liberated in particles of 3 mm than in particles of 6 mm.

Spiral separation using samples crushed to 1 and 0.5 mm showed a sharp increase in SE compared with those of jigging and DHIMS. The SE values obtained at 1 mm particle size varied from 7% to 31% while those obtained at 0.5 mm particle size varied from 23% to 44%. The high SE of spiral separation may be attributed to the improved liberation of Fe from the phosphate minerals. Taken together, the results reveal that spiral separation of particles 0.5 mm in size would result in efficient separation of Fe minerals from phosphate minerals.

4. Conclusions

(1) DHIMS of 6 and 3 mm non-metallic LD slag improved the Fe content of the magnetic concentrate by an absolute value of 4wt%–6wt%. However, the P content of the concentrate did not decrease significantly. These results reveal that DHIMS produces high concentrate yields with low separation efficiency. The poor liberation of Fe and P compounds may explain the low separation efficiency of the process.

(2) Jigging of 6 and 3 mm particles did not result in an appreciable reduction of the P content of the concentrate. The separation efficiency of jigging was inferior to that of DHIMS, and the former operation could not achieve less than 1wt% P in the concentrate.

(3) Spiral separation of both 1 and 0.5 mm particles showed good SE. The P content of the concentrate was reduced to as low as 0.75wt% with an Fe content upgrade to

about 45wt% in the 0.5 mm sample. The improved liberation of Fe from the slag particles may explain this result.

(4) Spiral separation is a technique that can potentially lower the P content and enrich the Fe content of non-metallic LD slag.

Acknowledgements

The authors thank the Research & Development Division and Management of Tata Steel Ltd. for their support and permission to publish this work. The authors also appreciate the helpful discussion and suggestions provided by Dr. Tamal Kanti Ghosh during the course of our research work on the dephosphorization of LD slag.

References

[1] I.Z. Yildirim and and M. Prezzi, Chemical, mineralogical, and morphological properties of steel slag, *Adv. Civ. Eng.*, 2011(2011), Art. No. 463638.

[2] X.R. Wu, G.M. Yang, L.S. Li, H.H. Lü, Z.J. Wu, and X.M. Shen, Wet magnetic separation of phosphorus containing phase from modified BOF slag, *Ironmaking Steelmaking*, 41(2014), p. 335.

[3] B. Das, S. Prakash, P.S.R. Reddy, and V.N. Misra, An overview of utilization of slag and sludge from steel industries, *Resour. Conserv. Recycl.*, 50(2007), p. 40.

[4] N. Menad, N. Kanari, and M. Save, Recovery of high grade iron compounds from LD slag by enhanced magnetic separation techniques, *Int. J. Miner. Process.*, 126(2014), p. 1.

[5] S. Radosavljevic, D. Milic, and M. Gavrilovski, Mineral processing of a converter slag and its use in iron ore sintering, *Magn. Electr. Sep.*, 7(1996), No. 4, p. 201.

[6] J. Geiseler, Use of steelworks slag in Europe, *Waste Manage.*, 16(1996), No. 1-3, p. 59.

[7] V. Ghai and W.H. Noseworthy, Resource recovery programs at Lake Erie Steel, *Iron Steel Eng.*, 1998, 75(5), p. 24.

[8] L.S. Ökvist, D.Q. Cang, Y.B. Zong, and H. Bai, The effect of BOF slag and BF flue dust on coal combustion efficiency, *ISIJ Int.*, 44(2004), No. 9, p. 1501.

[9] R. Panda, R.N. Karand, and C.R. Panda, Dephosphorization of LD slag by *Penicillium citrinum*, *The Ecoscan*, III(2013), Spec. Iss., p. 247.

[10] P. Chaurand, J. Rose, V. Briois, L. Olivi, J. Hazemann, O. Proux, J. Domas, and J. Bottero, Environmental impacts of steel slag reused in road construction: a crystallographic and molecular (XANES) approach, *J. Hazard. Mater.*, 139(2007), No. 3, p. 537.

[11] Y. Topkaya, N. Sevinç, and A. Günaydın, Slag treatment at Kardemir integrated iron and steel works, *Int. J. Miner. Process.*, 74(2004), No. 1-4, p. 31.

[12] H. Nashiwa, T. Mizuno, J. Ohi, and K. Katohgi, Effective use of returned LD slagand dolomite and operation with sub lance system, *Ironmaking Steelmaking*, 5(1978), p. 95.

[13] W.B. Dai, Y. Li, D.Q. Cang, Y.Y. Zhou, and Y. Fan, Effects of Sintering atmosphere on the physical and mechanical properties of modified BOF slag glass, *Int. J. Miner. Metall. Mater.*, 21(2014), No. 5, p. 494.

[14] K.K. Sharma, S. Swaroop, and D.S. Thakur, Recycling of LD slag through sinter route on direct charging in blast furnace at Bhilai Steel Plant, [in] *Proceedings of National Seminar on Pollution Control in Steel Industries*, Ranchi, 1993, p. 72.

[15] K. Morita, M.X. Guo, N. Oka, and N. Sano, Resurrection of the iron and phosphorus resource in steel-making slag, *J. Mater. Cycles Waste Manage.*, 4(2002), p. 93.

[16] S.M. Jung and Y.J. Do, Reduction behaviour of BOF slag by carbon in iron, *Steel Res. Int.*, 77(2006), p. 312.

[17] S.H. Huang, Y.Q. Wu, X.S. Liu, Z.R. Xu, and X.H. Lv, Experimentalstudy on gasification dephosphorization of converter slag with reduction by silicon, *Iron Steel*, 43(2008), No. 2, p. 31.

[18] H. Ono, A. Inagaki, T. Masui, H. Narita, T. Mitsuo, S. Nosaka, and S. Gohda, Removal of phosphorus from LD converter slag by floating of dicalcium silicate during solidification, *Tetsu-to-Hagane*, 66(1980), No. 9, p. 1317.

[19] K. Yokoyama, H. Kubo, K. Mori, H. Okada, S. Takeuchi, and T. Nagasaka, Separation and recovery of phosphorus from steelmaking slags with the aid of a strong magnetic field, *ISIJ Int.*, 47(2007), No. 10, p. 1541.

[20] H. Kubo, K.M. Yokoyama, and T. Nagasaka, Magnetic separation of phosphorus enriched phase from multiphase dephosphorization slag, *ISIJ Int.*, 50(2010), No. 1, p. 59.

[21] F.J. Doucet, Effective CO_2-specific sequestration capacity of steel slags and variability in their behaviour in view of industrial mineral carbonation, *Miner. Eng.*, 23(2010), No. 3, p. 262.

[22] A.S. Reddy, R.K. Pradhan, and S. Chandra, Utilization of basic oxygen furnace (BOF) slag in the production of a hydraulic cement binder, *Int. J. Miner. Process.*, 79(2006), p. 98.

[23] E.F. Wu, S. Pignolet-Brandom, and I. Iwasaki, Liberation analysis of slow cooled steel making slags: implications for phosphorus removal, [in] *Proceedings of the 1st International Conference on Processing Materials for Properties*, Honolulu, 1993, p. 153.

[24] D.Y. Wang, M.F. Jiang, C.J. Liu, Y. Min, Y.Y. Cui, J. Liu, and Y.C. Zhang, Enrichment of Fe-containing phases and recovery of iron and its oxides by magnetic separation from BOF slags, *Steel Res. Int.*, 83(2012), No. 2, p. 189.